# Chapter 3

# Tribological Behaviour Under Dry Environment

## 3.1. Introduction

Tribological behaviour of fiber reinforced composites depend on the orientation of fibres with respect to the sliding direction of counterface (i.e., whether parallel, antiparallel or normal) [153, 154]. It is very difficult to generalize the fibre orientation effect on the tribological performance to get the desired results. Different types of composites yield different results with the orientation of fibres. Theoretically, the friction behaviour of a composite material depends upon the area proportion and local friction coefficient of different constituents with respect to the counter surface [155]. The area proportion of different phases in a laminated composite change with the orientation of laminates. Most of the investigations focused on wear and friction performance of C/C and C/C–SiC composites dealt with a parallel orientation of laminates. Normal orientation effects are still not very clear. Besides this theoretical interpretation, when the materials are investigated experimentally, several other factors like formation and disruption of friction film, the involvement of wear debris, fracture of fibres etc. are also involved.

Tribological behaviour of C/C and C/C-SiC composites also depend on the counter surface material to a greater extent [125, 136]. Several researchers [156-158] had investigated the tribological behaviour of C/C and C/C-SiC composites using the parallel orientation of laminates in self-mated pairs. They have shown that in the case of C/C and C/C-SiC self-mated pair, the inset of friction film formation plays an important role. Friction film alleviates the effect of ploughing in case of C/C-SiC self-mated pair. The ease of formation and disruption of friction film depends on several factors like heat generation during testing,

debris interaction, braking energy, etc. The synergism among these factors depicts the surface conditions during testing. Surface conformity also affects the tribological behaviour of materials. C/C and C/C-SiC composites are mostly investigated with fully conformal surfaces. [16, 113, 124, 158-160]. Few researchers have conducted research using surfaces with low conformity [136, 161, 162]. The tests conducted on surfaces with full conformity differs from the tests conducted with low or non-conformal contacts [161]. To the best of our knowledge, tribological behaviour of C/C and C/C-SiC composites under non-conformal hertzian contacts have not been investigated yet. Further, most of the investigations on the sliding behaviour of C/C and C/C-SiC composites are based on high energy braking conditions. Sliding behaviour under low energy conditions has not been investigated to a significant extent.

Tribological behavior of a material is different in reciprocating sliding when compared with unidirectional sliding [163-167] due to variation in friction and wear mechanisms. In unidirectional sliding, sudden transition in friction regime doesn't take place whereas transition in friction regime takes place at the beginning of each stroke in case of reciprocating sliding [167]. Thus, the characteristics shown by reciprocating sliding are different from unidirectional sliding. Most of the investigations carried on the tribological behaviour of C/C and C/C-SiC composites are based on unidirectional sliding whether it is the pin on disk arrangement or disk on disk arrangement. According to our knowledge, tribological behavior of C/C and C/C-SiC composites under reciprocating motion with the variation of laminate orientation and surface conformity has not been investigated yet.

Thus in this chapter, dry sliding behaviour of C/C and C/C-SiC composites had been investigated for unidirectional as well as reciprocating sliding. Two orientations of laminates

were considered, i.e. normal and parallel orientation with respect to the sliding direction of counterface. Theoretically, overall friction and wear behaviour of a composite depends upon the local friction and wear response of its different constituents whose proportions change with the orientation of laminates. Thus, the preliminary guess was that the composites with parallel orientation of laminates should show higher friction coefficient and wear resistance because of the higher area proportion of fibres on the contact surface. But the analysis showed that several other factors were also involved. Further, low conformity and non-conformal hertzian contacts were considered to analyze the surface conformity effect. The tests were conducted on pin/ball on disk/plate tribometer. Most of the earlier investigations on tribological behaviour of C/C and C/C-SiC composites were carried out using inertial type dynamometer. Tests conducted using open type configuration (pin/ball on disk/plate tribometer) differs from tests conducted using closed type configuration (inertial type dynamometer).

### 3.2. Materials and Synthesis

The processing steps for the manufacturing of cross plied ($0^o/90^o$) C/C and cross plied ($0^o/90^o$) C/C-SiC composites are shown in Fig. 3.1. Carbon/carbon (C/C) composites were received from Division of Space Propulsion, Institute of Space and Astronautical Science, 3-1-1 Yoshinadai, Sagamihara-shi, Kanagawa-ken, Japan. The 2D woven fabric C/C composites were manufactured by reinforcing plain woven cloths of carbon fibres (containing high strength carbon fibres with 7 μm diameter) in phenolic resin. The resulting carbon fibre reinforced polymer (CFRP) composite was carbonized at 1000 $^oC$ and densified by repeated impregnation of phenolic resin in the vacuum, and carbonization (upto 6 cycles). Finally, the resulting composite was heat-treated at 1500 $^oC$. The obtained C/C composite

contained 50% carbon fibres by volume and 50% carbon matrix. C/C composite was having a density of 1.8 g/cm$^3$.

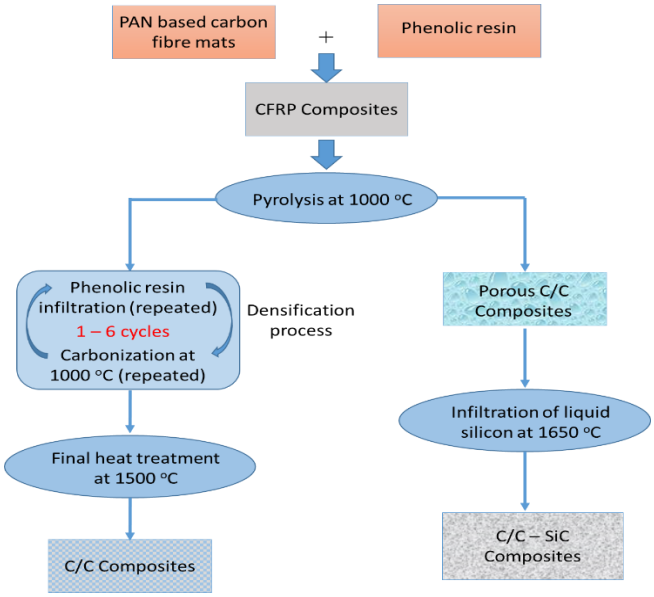


Fig. 3.1. Processing of C/C and C/C-SiC composites.

Carbon/carbon-silicon carbide (C/C – SiC) composites were received from MPA, University of Stuttgart, Germany. Porous cross plied ($0^o/90^o$) C/C composites were used as preform for C/C-SiC composites. The porous C/C preforms were prepared by the method as shown in Fig. 3.1 and then siliconized by liquid silicon infiltration (LSI) process. The preforms were heated in vacuum to the temperature of 1650 $^o$C. The molten silicon (melting point 1410 $^o$C) was infiltrated through the heated preforms. Molten silicon can enter the material only through micro-delaminations and segmentation cracks. Molten silicon reacted with the carbon matrix and formed silicon carbide. The obtained C/C–SiC composites contained about 38% of silicon carbide and 2% free silicon by volume. The resulting C/C-SiC composites were having a density of 1.85 g/cm$^3$.

After fabrication, composites were prepared in the form of cylindrical pins, square plates, and circular disks. To prepare cylindrical pins and circular disks, the composite samples were

firstly cut in the square section of required dimensions using diamond cutter. The square sections were then manually formed to circular shape using emery paper of different grades, i.e. 400, 1000 and 1200. The pins were prepared for both normal as well as for parallel orientation of laminates whereas disks and plates were prepared for only parallel orientation of laminates. The diameter of the composite pins was prepared to 9 mm and the diameter of the disks was prepared to 80 mm. To prepare square plates, composite samples were cut in square section of required dimensions using diamond cutter and then polished against emery paper of 1000 grade. The side of the resulting square plate was 50 mm.

### 3.3. Sliding Wear Tests

#### 3.3.1. Unidirectional Sliding

Friction and wear characteristics of C/C and C/C – SiC composites were investigated against chrome steel counterface. In case of low conformity contacts and non-conformal hertzian contacts, the disk and the ball were made of chrome steel respectively, which contained 13% chromium and 1.6% carbon. The hardness of the chrome steel was 62 HRc. The testing arrangement used for low conformity contacts and non-conformal hertzian contacts was the pin on disk and ball on disk tribometer, respectively. The pin on disk and ball on disk testing was performed on the same machine (TR-20LE-PHM 400, DUCOM, Bangalore, India). Samples, disk, and balls were cleaned using acetone before starting the tribological testing. The surface roughness ($R_a$) of the chrome steel disk was 0.4 µm before starting the tests.

The samples were firstly tested for the normal orientation of laminates (designated as C/C normal and C/C – SiC normal). For this, the orientation of the fibres was kept normal to the counter surface as shown in Fig. 3.2. The diameter of the prepared composite pins was 9 mm. Sliding wear tests were conducted at five different loads (i.e., 20 N, 30 N, 40 N, 50 N, 60 N

keeping sliding velocity fixed at 2 m/s) and five sliding velocities (i.e., 1 m/s, 1.5 m/s, 2 m/s, 2.5 m/s, 3 m/s keeping load fixed at 20 N). The tests were conducted for a total sliding distance of 5400 m at ambient conditions. Before starting the tests for low conformity contacts, composites pins were slid against the counter surface for a sliding distance of 4000 m to ensure the maximum conformity during testing. The frictional force was continuously recorded through data acquisition system. Wear loss was obtained by weighing the samples before and after the wear test using electronic weighing balance (DENVER INSTRUMENT, SI-234).

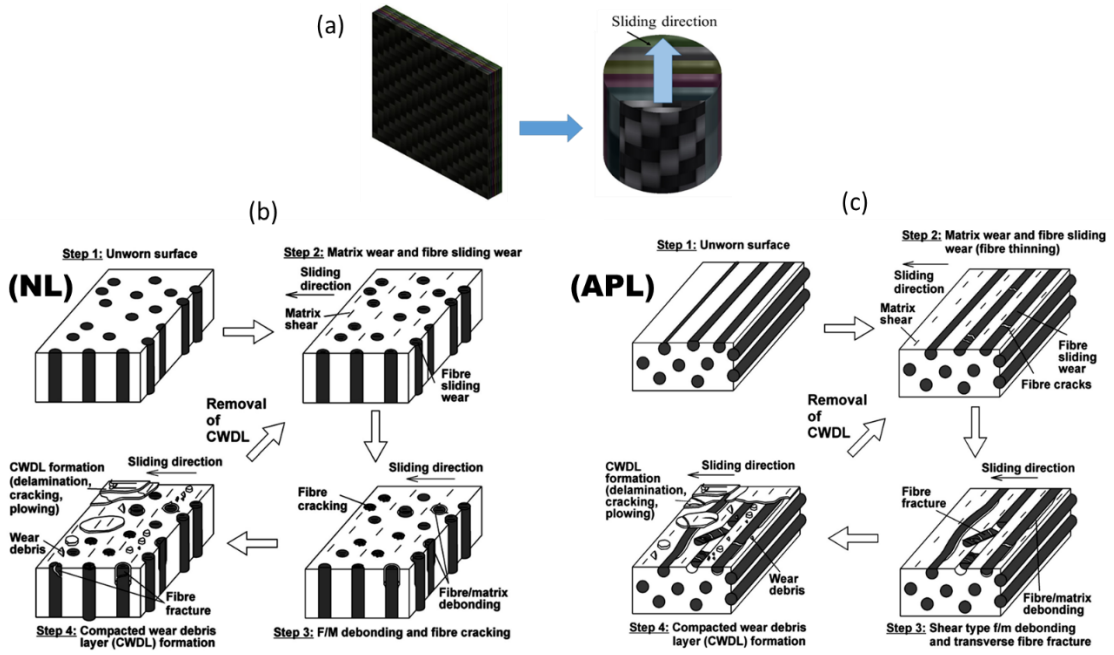


Fig. 3.2. Schematic showing (a) composite pin with normal orientation of laminates, and representative wear mechanisms in (b) normal (NL) and (c) anti-parallel (APL) direction of fibres. Panel (b) and (c) are reproduced from ref. [154].

After testing the samples for normal orientation of laminates, samples were tested for parallel orientation of laminates (designated as C/C parallel and C/C – SiC parallel). Due to insufficient thickness of composites having parallel laminates, a pin holder made of mild

steel was used so that it can be fitted into the fixture of the wear test rig for testing. The inner diameter of the pin holder was 9 mm, and the outer diameter was 11 mm. The procedure followed for friction and wear testing was the same as in the case of normal orientation of laminates. Fig. 3.3 shows the sliding direction of the composite with respect to counter surface in case of parallel orientation of laminates.

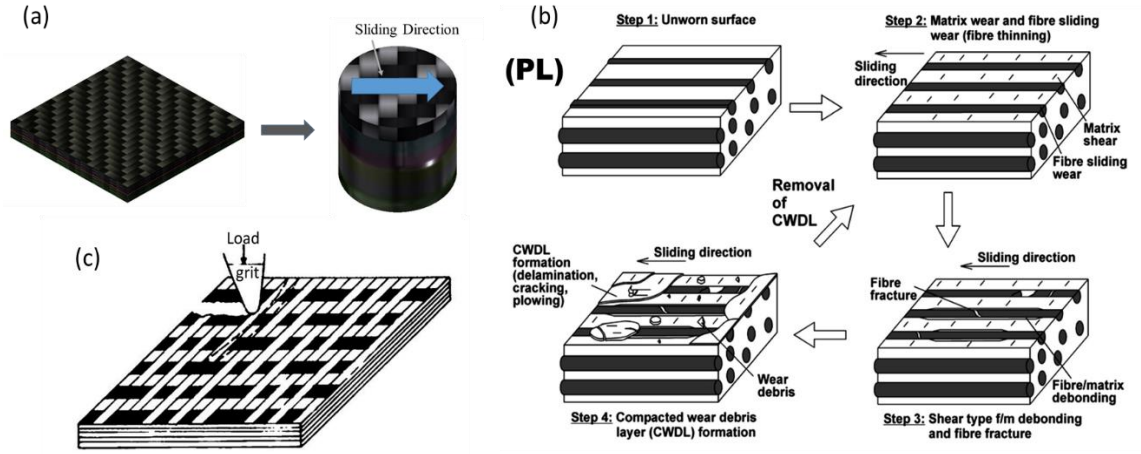


Fig. 3.3. Schematic showing (a) composite pin with parallel orientation of laminates, (b) wear mechanisms in parallel (PL) direction of fibres, and (c) grit abrasion. [154]

After testing the samples for parallel orientation of laminates, testing for non-conformal hertzian contacts was performed. For non-conformal hertzian contacts, ball on disk (sphere on the plane) arrangement was used. The disk was a composite sample having the parallel orientation of laminates (designated as C/C disk and C/C – SiC disk). The ball was made of chrome steel having a diameter of 10 mm. The rest of the procedure was the same as in case of normal orientation of laminates.

The results from low conformity contacts and non-conformal contacts were reported against applied normal load and sliding velocity. But the normal pressure generated in case of low conformity contacts was different from non-conformal hertzian contacts at the same load. To simplify the data for comparison purpose, results were plotted against the normal load. For

low conformity contacts, the pressures (calculated by applied load/apparent contact area) corresponding to the loads of 20 N, 30 N, 40 N, 50 N and 60 N was 0.31 MPa, 0.47 MPa, 0.63 MPa, 0.78 MPa, and 0.94 MPa respectively. For non-conformal hertzian contacts, the average hertzian contact pressure (calculated by hertzian contact stress equations) corresponding to loads of 20 N, 30 N 40 N, 50 N and 60 N was 0.49 GPa, 0.57 GPa, 0.63 GPa, 0.67 GPa, and 0.71 GPa respectively in case of C/C composites. There was a very small difference between contact pressures in case of C/C-SiC composites as compared to C/C composites. So contact pressures for C/C composites are written only. Each test was carried out four times for the same set of variables and the average value from four tests was reported. The temperature of ambient and relative humidity at the time of testing was 32 +/- 2 $^{o}$C and 64% respectively.

### 3.3.2. Reciprocating Sliding

Chrome steel was used as counterface to carry out reciprocating wear testing (plate in case of pin/plate arrangement and ball in case of ball/plate arrangement) as in case of unidirectional sliding. Wear tests were performed on reciprocating sliding wear test rig (TE 200ST, Magnum Engineers, Bangalore, India). Each test was performed at 5 Hz frequency and for 13500 cycles. Stroke length was kept as 3 mm. Friction coefficient and wear loss were investigated. To investigate wear loss, samples were weighed before and after the test using a weighing machine (Model No.- RA310, Roy Electronics, Varanasi, India). Prior to testing, samples were cleaned using acetone. The effect of load on reciprocating wear behavior was also investigated. The load was varied ranging 50 N, 60 N, 70 N, 80 N and 90 N. It can be observed that in case of reciprocating sliding, normal load was varied from 50 N to 90 N in the steps of 10 N whereas in case of reciprocating sliding, normal load was

varied from 20 N to 60 N in the steps of 10 N. This was done because wear loss was almost negligible up to 40 N load in case of reciprocating sliding. Variation of laminate orientation and surface conformity was carried out the same way as in case of unidirectional sliding.

### 3.3.3. Wear Mechanisms

It can be observed from Figs. 3.2 (b), 3.2 (c) and 3.3 (b) that the tribological interactions involve normal (NL), antiparallel (APL), and parallel (PL) directions of fibres. It is clear from Fig. 3.2 (a) that normal orientation of laminates involve fibres in NL and APL directions, whereas Fig. 3.3 (a) shows that parallel orientation of laminates involves fibres in PL and APL directions. The schematic illustrations showing representative wear mechanisms is shown in Figs. 3.2 (b), 3.2 (c) and 3.3 (b). It can be observed from Figs. 3.2 (b), 3.2 (c) and 3.3 (b) that fibre/matrix debonding occurs due to the shear and tension type loading. Furthermore, grit abrasion may also occur (as shown in Fig. 3.3 (c)) which results in breakage of fibres and hence, the debonding of fibre from matrix becomes easy. If fibre/matrix debonding takes place, the local separation initiates additional fibre cracking and wear debris formation. The compaction of pulverized wear debris form compacted wear debris layer (CWDL, also called friction film) which covers the surface. Due to third body particles (such as hard particles in wear debris and broken fibers), the disruption of CWDL may also occur. Thus, formation and disruption of CWDL may take place simultaneously. The detailed discussion of representative wear mechanisms shown in Figs. 3.2 (b), 3.2 (c) and 3.3 (b), and the factors dictating them is elaborated in the discussion part of the present and subsequent chapters.

### 3.4. Scanning Electron Microscopy

After completion of friction and wear testing, worn surfaces were analyzed using a scanning electron microscope (SEM) to study wear mechanisms. A ZEISS EVO 18 RESEARCH, 20 kV scanning electron microscope was used to analyze worn surfaces. To analyze the worn surface of composite pins with normal orientation of laminates, the worn surface were cut from the pin in the form of circular tablets having 5 mm thickness. To analyze disks, the worn portion of the disks were cut out in the dimension of 5 mm X 5 mm. After preparing the samples for scanning electron microscopy, samples were mounted on the sample holder of SEM and analyzed.

### 3.5. Results and Discussion

#### 3.5.1. Unidirectional Sliding

##### 3.5.1.1. Friction response

Representative plots of friction coefficient versus time for C/C and C/C – SiC composites with normal and parallel orientation of laminates are shown in Figs. 3 and 4.

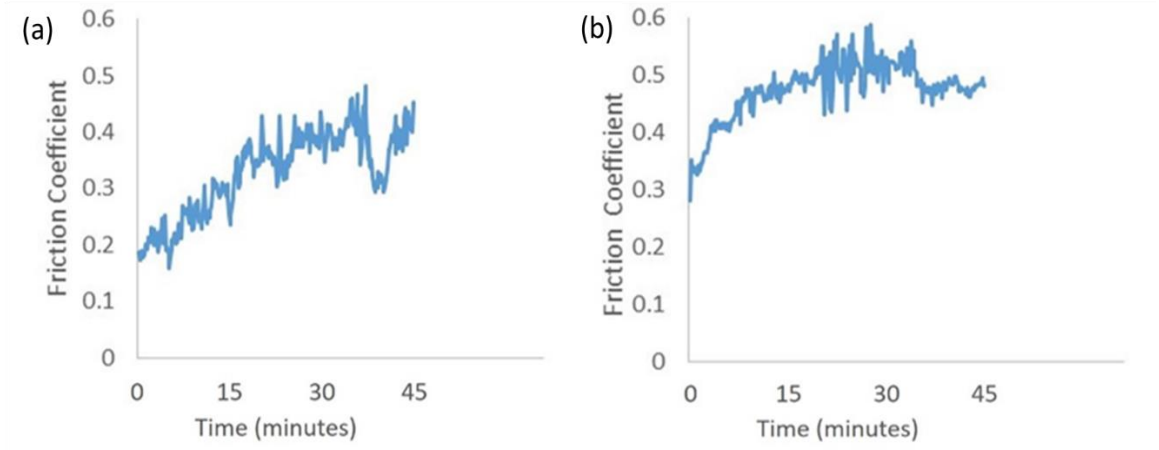


Fig. 3.4. Representative plot for variation of friction coefficient with time plotted for 40 N load and 2 m/s sliding velocity with normal orientation of laminates (a) C/C composites, (b) C/C – SiC composites.

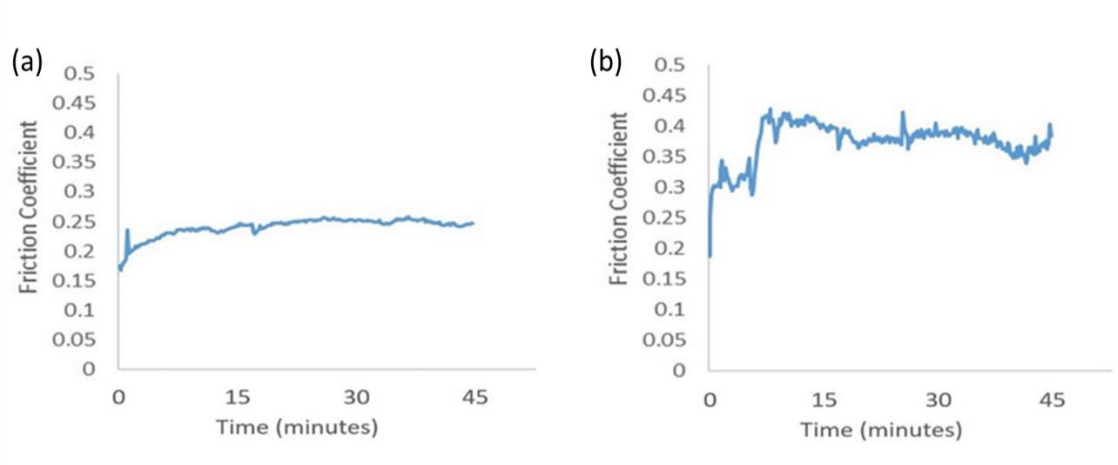


Fig. 3.5. Representative plot for variation of friction coefficient with time plotted for 20 N load and 2 m/s sliding velocity with parallel orientation of laminates (a) C/C composites, (b) C/C – SiC composites.

It can be observed from Figs. 3.4 and 3.5 that friction coefficient increased with time. This rise was attributed to an increase in temperature with time, as indicated by a panel on tribometer. The increase in temperature enhanced adhesion and abrasion of contact conjunctions and asperities on the contact surface [22]. However, fluctuations in case of composites having the normal orientation of laminates were more as compared to composites having the parallel orientation of laminates due to more surface porosity in case of parallel laminates. Thus the wear debris filled the pores and formed a smooth surface which led to the stability of friction coefficient as the time elapsed.

It can be observed in Fig. 3.6 that mean friction coefficient (as indicated by computer interface of tribometer) for C/C normal increased with increase in load beyond 30 N. When the load was varied from 20 N to 30 N, mean friction coefficient decreased for C/C normal. For C/C parallel, friction coefficient increased when the load was varied from 20 N to 30 N and after that decreased up to 50 N load. Friction coefficient for C/C – SiC normal and C/C – SiC parallel generally increased with increase in load.

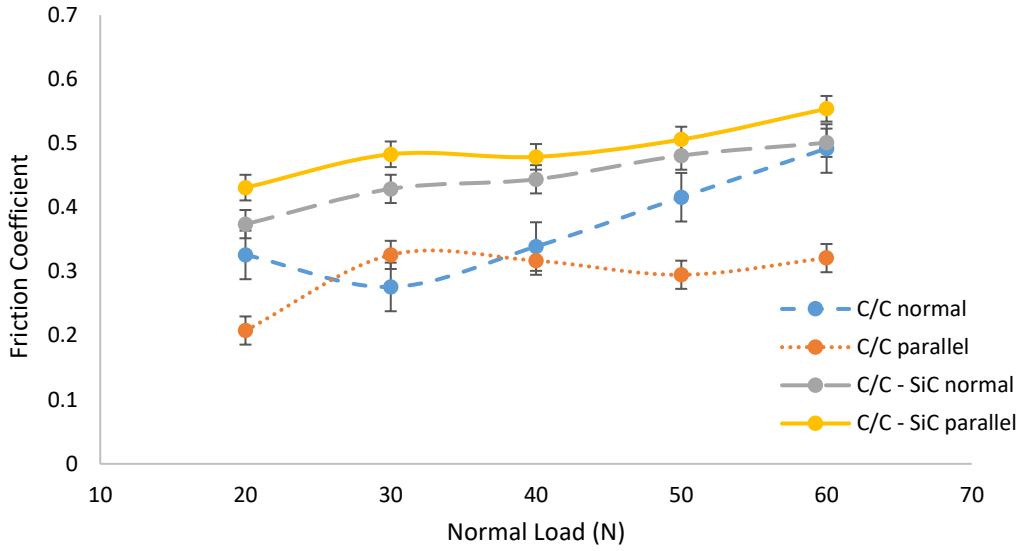


Fig. 3.6. Variation of friction coefficient with normal load for low conformity contacts of C/C normal, C/C parallel, C/C-SiC normal and C/C-SiC parallel composites.

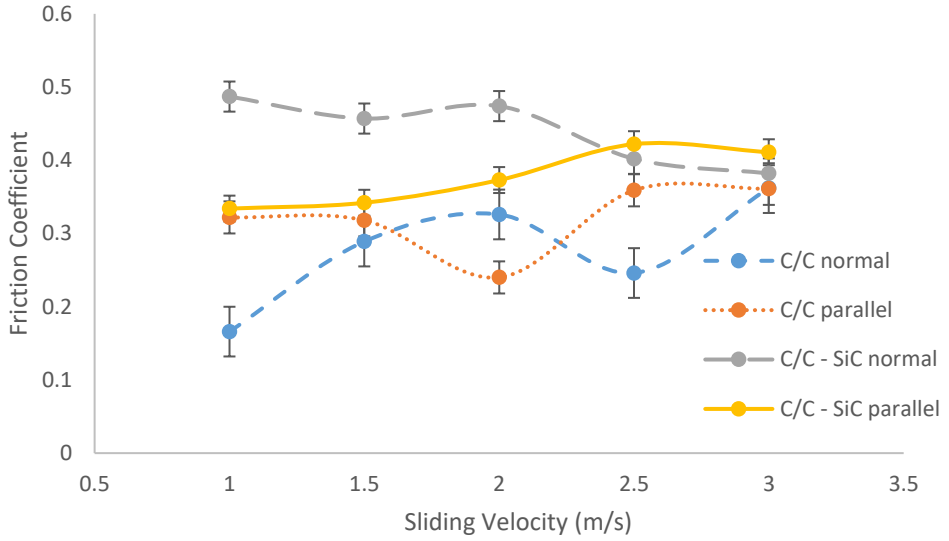


Fig. 3.7. Variation of friction coefficient with sliding velocity for low conformity contacts of C/C normal, C/C parallel, C/C-SiC normal and C/C-SiC parallel composites.

It can be observed from Fig. 3.7 that friction coefficient for C/C normal increased with an increase in sliding velocity up to 2 m/s. After that, it decreased for 2.5 m/s sliding velocity and again increased for 3 m/s sliding velocity. For C/C parallel, friction coefficient first

decreased up to 2 m/s velocity and after that increased. Friction coefficient of C/C – SiC normal decreased with an increase in sliding velocity whereas friction coefficient of C/C – SiC parallel increased with an increase in sliding velocity.

C/C composites showed an increase in friction coefficient up to 30 N load and decreased after that, in the case of non-conformal hertzian contacts as can be observed from Fig.3.8. However for C/C–SiC disk, friction coefficient increased with increase in load. The friction coefficient of C/C – SiC disk was more than that of C/C disk at all tested loads.

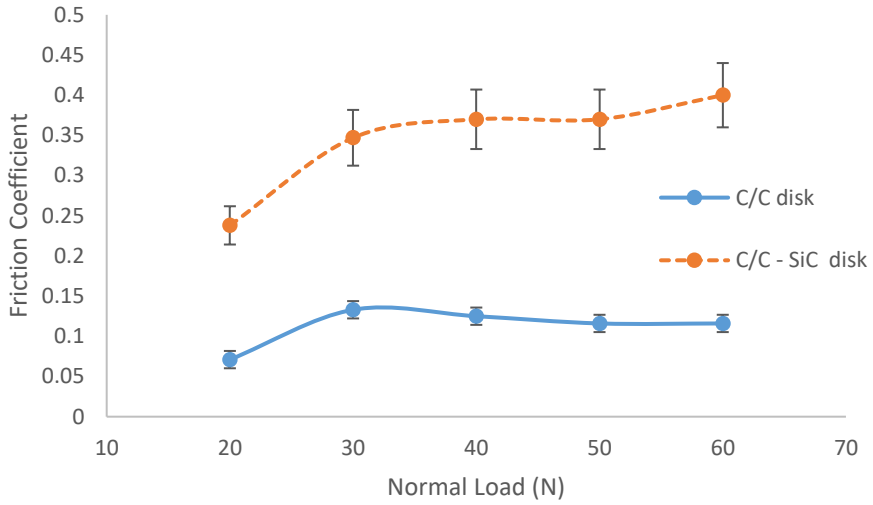


Fig. 3.8. Variation of friction coefficient with normal load for non-conformal hertzian contacts of C/C and C/C-SiC disks.

It can be observed from Fig. 3.9 that friction coefficient was almost constant for C/C disk at all tested velocities. However for C/C- SiC disk, friction coefficient first increased up to 2 m/s sliding velocity and then decreased after that. Friction coefficient of C/C – SiC disk was more than that of C/C disk for all tested velocities.

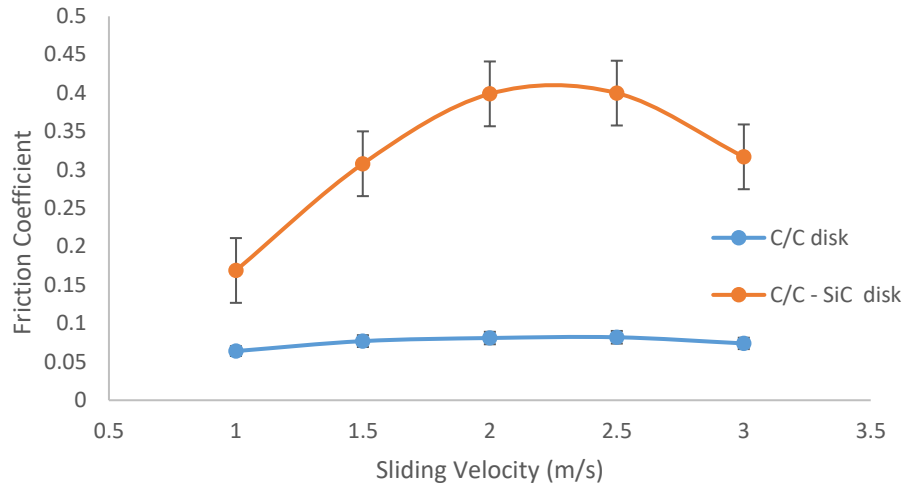


Fig. 3.9. Variation of friction coefficient with sliding velocity for non-conformal hertzian contacts of C/C and C/C-SiC disks.

### 3.5.1.2. Wear behaviour

Wear behaviour of composites was obtained by determining the wear loss. It can be observed from Fig. 3.10 that wear loss of all composites increased with increase in load. However, except C/C normal, the rise was steep for all when the load was increased from 50 N to 60 N.

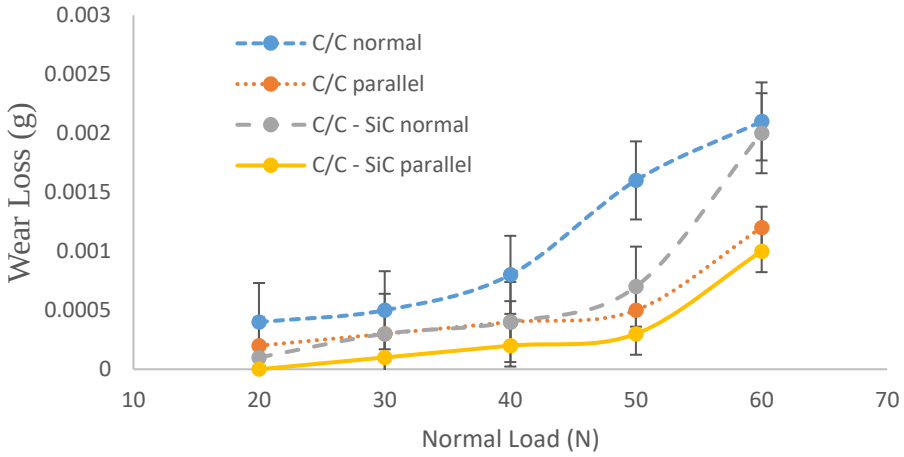


Fig. 3.10. Variation of wear loss with load for low conformity contacts of C/C normal, C/C parallel, C/C-SiC normal and C/C-SiC parallel composites.

For C/C normal, the rise was steep when the load was increased from 40 N to 50 N. Wear resistance of C/C parallel was almost same as C/C – SiC normal up to 40 N load. Wear loss of C/C – SiC parallel was negligible up to 20 N load. Wear resistance of C/C – SiC parallel was highest.

It can be observed from Fig. 3.11 that wear loss of C/C normal and C/C – SiC normal first increased with sliding velocity and decreased after that, as the sliding velocity was increased. However, for C/C parallel and C/C – SiC parallel, wear loss first decreased and afte increased afterwards.

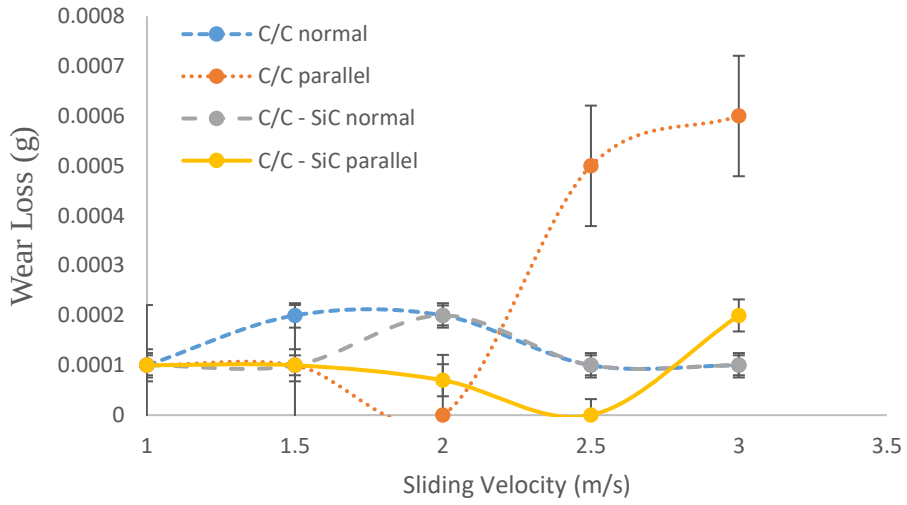


Fig. 3.11. Variation of wear loss with sliding velocity for low conformity contacts of C/C normal, C/C parallel, C/C-SiC normal and C/C-SiC parallel composites.

Wear loss of C/C normal and C/C – SiC normal was lowest at high sliding velocity.

It can be observed from Fig. 3.12 that wear loss of C/C disk was more than that of C/C – SiC disk.

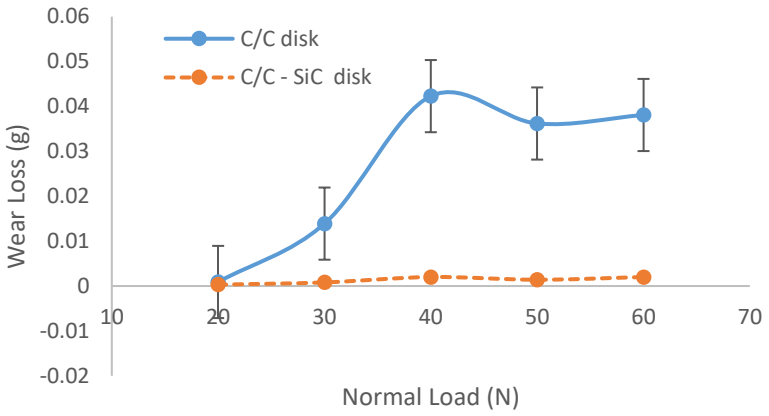


Fig. 3.12. Variation of wear loss with load for non-conformal hertzian contacts of C/C and C/C-SiC disks.

The wear loss for both C/C and C/C – SiC disks first increased up to 40 N load and then decreased at 50 N load. After that wear loss again increased for both C/C disk and C/C – SiC disks.

It can be observed from Fig. 3.13 that wear loss of C/C disk was more than that of C/C – SiC disk at all tested velocities.

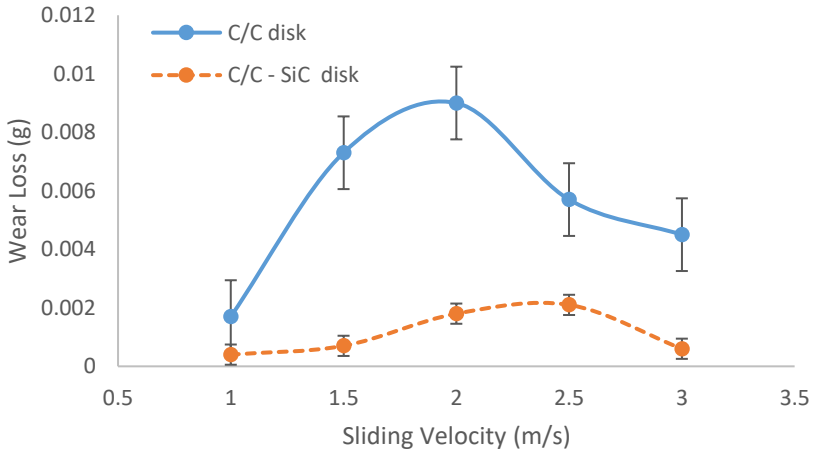


Fig. 3.13. Variation of wear loss with sliding velocity for non-conformal hertzian contacts of C/C and C/C-SiC disks.

Wear loss for C/C disk first increased up to 2 m/s sliding velocity and decreased after that. However, for C/C – SiC disk, wear loss increased up to 2.5 m/s sliding velocity and then decreased.

### 3.5.1.3. Discussion

When the load was increased from 20 N to 30 N in case of C/C normal, wear debris got pulverized and compacted and formed friction film on the surface of the composite which led to decrease in friction coefficient. However, when the load was increased beyond 30 N, friction coefficient increased. This can be attributed to the accelerated formation and disruption rate of friction film at higher loads. Disruption rate was more than the formation rate. Simultaneous formation and disruption of friction film can be observed in Fig. 3.14 (a).

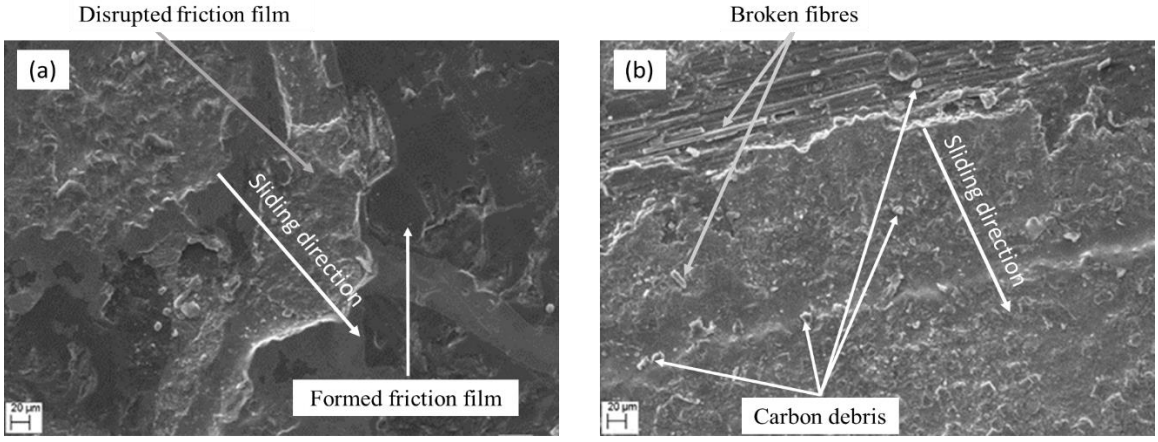


Fig. 3.14. SEM images showing C/C normal tested at (a) 40 N load and 2 m/s sliding velocity, and (b) 20 N load and 3 m/s sliding velocity.

As the sliding velocity was increased, friction coefficient of C/C normal first increased up to 2 m/s sliding velocity. After that, it decreased for 2.5 m/s and again increased for 3 m/s. The first rise in friction coefficient was due to the increase in breaking energy which led to rapid desorption of water vapour and oxygen from the contact surface [16, 168]. When the sliding velocity was increased beyond 2 m/s, further increase in braking energy led to increase in temperature due to which pulverization and compaction of wear debris were easy and continuous friction film was formed on the surface. This decreased the friction coefficient at 2.5 m/s. Again increasing the sliding velocity led to the accelerated ejection of wear debris due to centrifugal force [161] which again increased the friction coefficient. Fig. 3.14(b) shows C/C normal tested at 3 m/s sliding velocity. Some broken fibres (in the form of small fragments) due to grit abrasion, and carbon debris can be observed. However, very less friction film was formed.

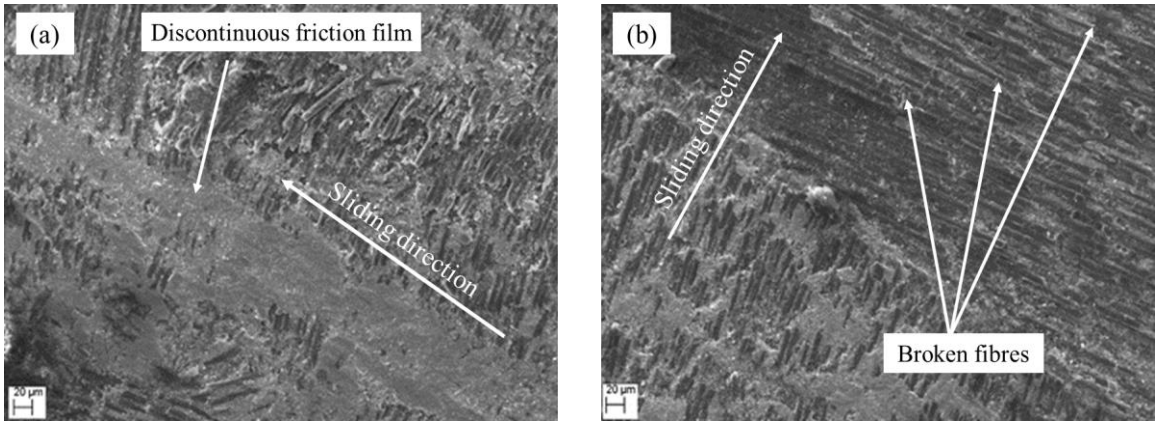


Fig. 3.15. SEM images showing C/C parallel tested at (a) 60 N load and 2 m/s sliding velocity, and (b) 20 N load and 2.5 m/s velocity.

In the case of C/C parallel, the increase in friction coefficient up to 30 N load was due to deeper penetration asperities with the increased load which increased resistance to sliding. However as the load was increased further, the formation of friction film led to a decrease in friction coefficient. Further increase in load led to rapid formation and disruption of friction film which led to an increase in friction coefficient. Discontinuous friction film at 60 N load can be observed from Fig. 3.15(a).

Formation of friction film at low sliding velocity and its accelerated rate of formation and disruption due to spreading of wear debris at higher sliding velocities [161] describes the nature of friction coefficient with the increase in sliding velocity. Fig. 3.15(b) shows C/C parallel at 2.5 m/s velocity and 20 N load. It can be observed that at high sliding velocity, wear debris didn't pile up much on the surface. Some broken fibres were observed.

C/C normal showed opposite friction behaviour as compared to C/C parallel. In the case of C/C parallel, the formation of smooth surface was easy due to more surface porosity and filling up of pores by the generated wear debris. However, in case of normal orientation of laminates, formation, and disruption of friction film affected the friction film when load and sliding velocity were varied.

Friction coefficient of C/C – SiC normal and C/C – SiC parallel increased as the load was increased. This was attributed to the deeper penetration of hard SiC and second phase Si particles into the counterface as the load was increased [113, 125, 131]. There is also free silicon in case of C/C –SiC composites which plasticize at higher load and led to adhesion at higher loads, thereby increased friction coefficient [113]. Fig. 3.16(a) shows C/C-SiC normal tested at 30 N load and 2 m/s sliding velocity. SiC particles in wear debris were observed.

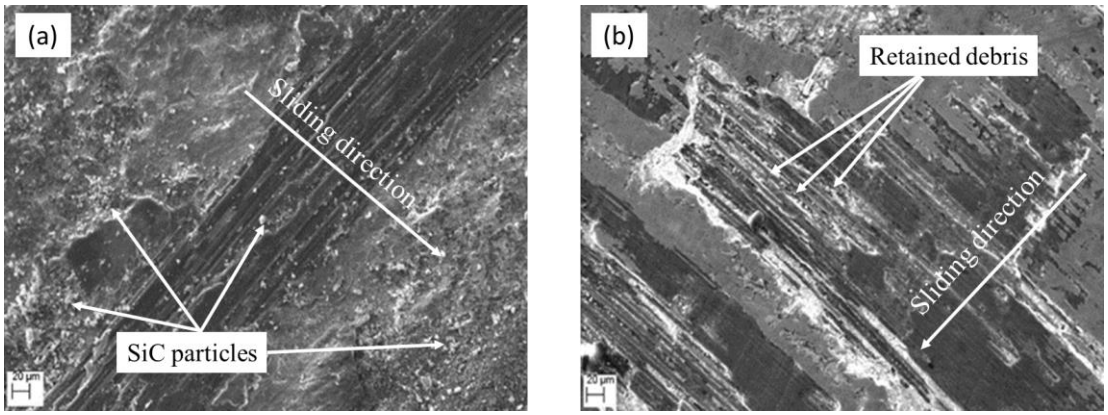


Fig. 3.16. SEM images showing composites tested at 30 N load and 2 m/s sliding velocity (a) C/C-SiC normal, (b) C/C-SiC parallel.

Fig. 3.16(b) shows C/C-SiC parallel tested at 30 N load and 2 m/s velocity. Debris retention in between the fibres can be observed. This hard debris increased the friction coefficient as the load was increased. At higher loads, fibre breakage due to repeated sliding in one direction was observed.

C/C-SiC normal showed the decrease in friction coefficient when the sliding velocity was increased. As sliding velocity was increased, the formed wear debris spread more easily on the surface. Debris contained hard SiC and second phase Si particles. SiC and second phase Si particles can't be cut easily. The spread debris rolled in between the contact surfaces. Fig. 3.17(a) shows C/C-SiC normal tested at 3 m/s sliding velocity and 20 N load. Wear debris can be observed.

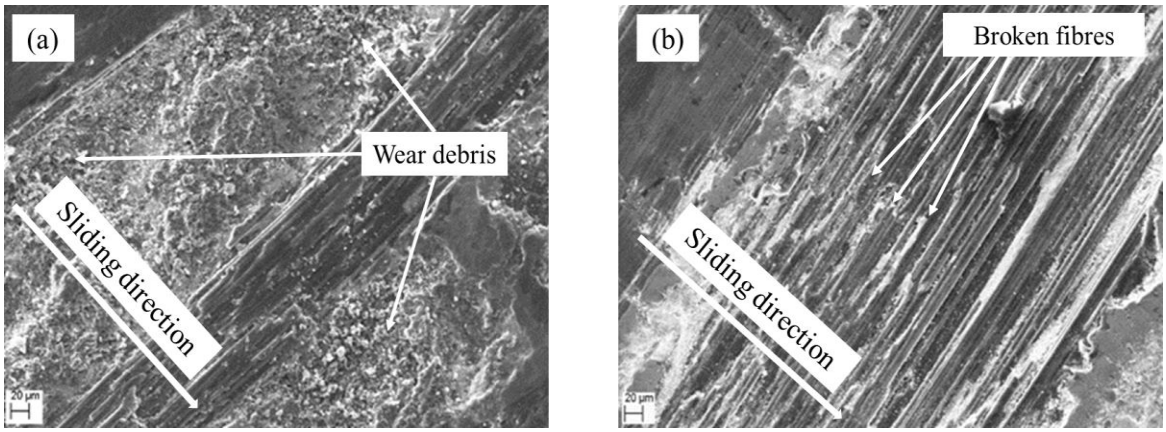


Fig. 3.17. SEM images showing (a) C/C-SiC normal tested at 3m/s sliding velocity and 20 N load, and (b) C/C-SiC parallel tested at 1.5 m/s sliding velocity and 20 N load.

Friction coefficient of C/C – SiC parallel increased when the sliding velocity was increased. This was due to the resistance provided by breaking of fibres [161]. As the sliding velocity was increased, the particles which were ejected from the surface slid from the surface due to centrifugal force [136], and fibres directly came in contact with the counterface. The increase in braking energy due to the increase in sliding velocity led to breakage of fibres. More fibres broke at higher velocities which increased friction coefficient. Broken fibres can be observed in Fig. 3.17(b).

C/C – SiC parallel generally showed more friction coefficient as compared to C/C – SiC normal. Friction coefficient of composites depends on the interaction and local friction coefficient of different constituents [155]. C/C-SiC parallel contained more proportion of SiC as compared to C/C-SiC normal. Thus, C/C-SiC exhibited higher friction coefficient as compared to C/C-SiC normal.

Friction coefficient of C/C disk first increased and then decreased a bit when the load was increased in case of non-conformal hertzian contacts. This was attributed to the easy formation of friction film due to localized stress regions. However, for C/C-SiC disk, the formation of friction film took place at moderate loads. But at high loads, SiC disrupted the formed friction film and abraded the steel ball which increased friction coefficient at high loads. The difference between friction coefficient values from low conformity contacts and non-conformal hertzian contacts was large in case of C/C composites as compared to C/C-SiC composites. The friction coefficient value was less in case of non-conformal hertzian contacts as compared to low conformity contacts because the contact area in case non-conformal contacts was very much petite and generation of high and localized stresses led to the easy formation of friction film which decreased friction coefficient.

Wear loss of C/C and C/C-SiC composites increased with increase in load whether it was the normal or parallel orientation of laminates. It was observed that the composites with a parallel orientation of laminates showed less wear loss as compared to composites with normal orientation of laminates. This was due to more surface porosity in case of parallel orientation of laminates. Wear debris filled the pores and formed a smooth surface. However, at higher sliding velocities, wear loss of composites having the parallel orientation of laminates was more. This was because of the easy spreading of wear debris at high sliding velocities due to which smooth surface formation didn't take place. The areal proportion of carbon fibres was more in case of parallel orientation of laminates. The local friction coefficient of carbon fibres is more as compared to carbon matrix. Thus, a higher proportion of carbon fibres in case of parallel orientation led to a higher value of friction coefficient and hence increased the temperature of contact surfaces which led to increase in wear.

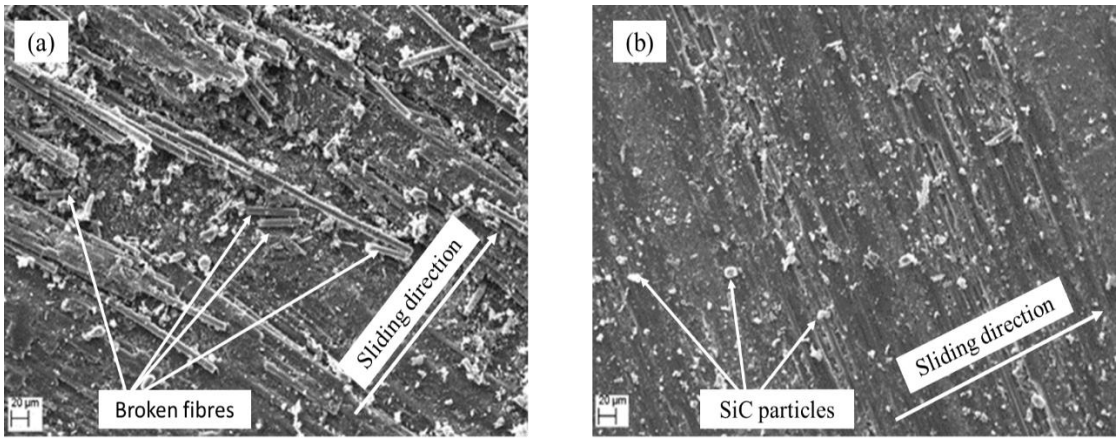


Fig. 3.18. SEM images showing composites tested at 40 N load and 2 m/s sliding velocity (a) C/C disk, and (b) C/C-SiC disk.

Wear loss of C/C composites was more as compared to C/C-SiC composites in non-conformal hertzian contacts. Fig. 3.18(a) shows C/C disk tested at 40 N load and 2 m/s sliding velocity in non-conformal hertzian contacts. It was observed that due to the formation of grooves in the vicinity of the contact area, wear debris didn't get escaped much. Broken fibres can also be observed. Thus at higher load, some wear debris pulverized, and the unpulverized particles acted as the third body which rolled in between the contact surfaces and decreased the wear loss at higher loads. In the case of C/C-SiC composites, the wear debris contained hard SiC particles as can be observed in Fig. 3.18(b).

SiC particles are hard to cut and pulverize even at high loads. Thus wear loss of C/C-SiC composites was lower than C/C composites in non-conformal hertzian contacts.

Wear loss in case of non-conformal hertzian contacts was more as compared to low conformity contacts due to the generation of high and localized stress regions. The pressure corresponding to the same load (as in low conformal contacts) was very much high which led to increased wear loss.

### 3.5.2. Reciprocating Sliding

#### 3.5.2.1. Friction response

Fig. 3.19 shows the variation of friction coefficient with time in case of C/C composites. It can be observed that fluctuations in case of C/C normal were more as compared to C/C parallel. The friction coefficient of C/C normal first increased with time and then decreased. However, friction coefficient of C/C attained a value and was almost constant at that value. The friction coefficient of C/C parallel was more stable.

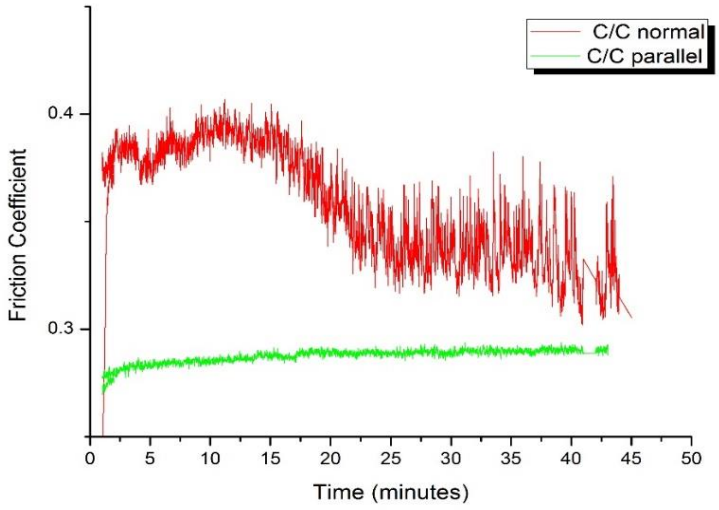


Fig. 3.19. A representative plot for variation of friction coefficient with time for C/C composites (plotted for 70 N load).

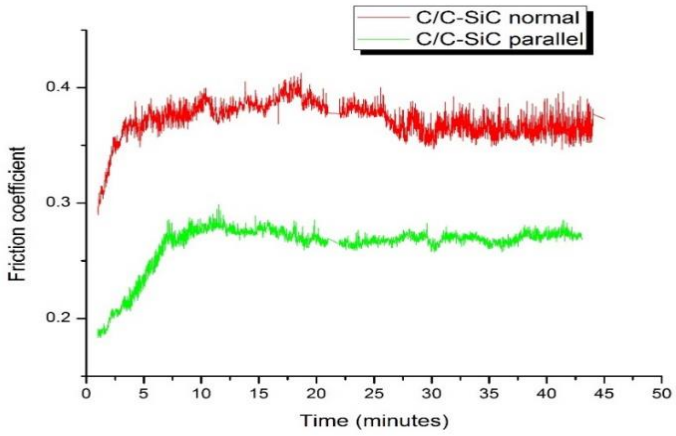


Fig. 3.20. A representative plot for variation of friction coefficient with time for C/C-SiC composites (plotted for 70 N load).

It can be observed from Fig. 3.20 that friction coefficient of C/C-SiC normal was more stable as compared to C/C normal. For C/C-SiC composites also, friction coefficient with a parallel orientation of laminates was more stable than for normal orientation of laminates.

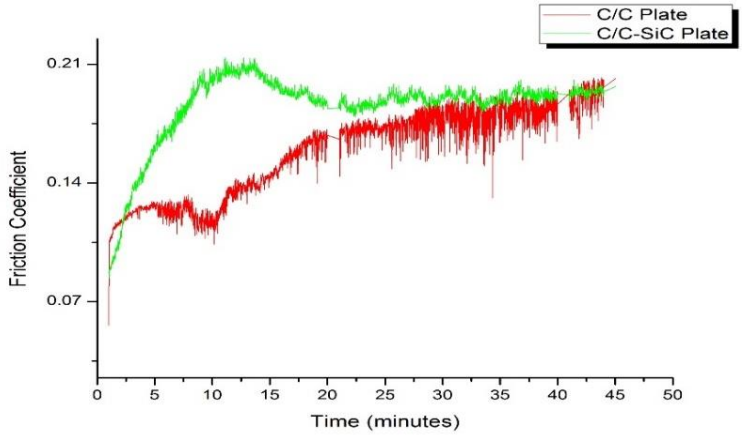


Fig. 3.21. A representative plot for variation of friction coefficient with time for C/C and C/C-SiC composites in non-conformal hertzian contacts (plotted for 70 N load).

It can be observed from Fig. 3.21 that in case of non-conformal hertzian contacts, the friction coefficient of C/C composites first decreased with time and after that increased. For C/C-SiC

composites, friction coefficient first increased and decreased after that. Friction coefficient in case of non-conformal hertzian contacts was low as compared to low conformity contacts. Fig. 3.22 shows the variation of friction coefficient with the load. It can be observed from Fig. 3.22 that friction coefficient of C/C parallel and C/C-SiC normal first increased with increase in load and after that decreased whereas friction coefficient of C/C-SiC parallel first decreased with increase in load and after that increased. The friction coefficient of C/C normal showed increasing trend up to 90 N loading conditions.

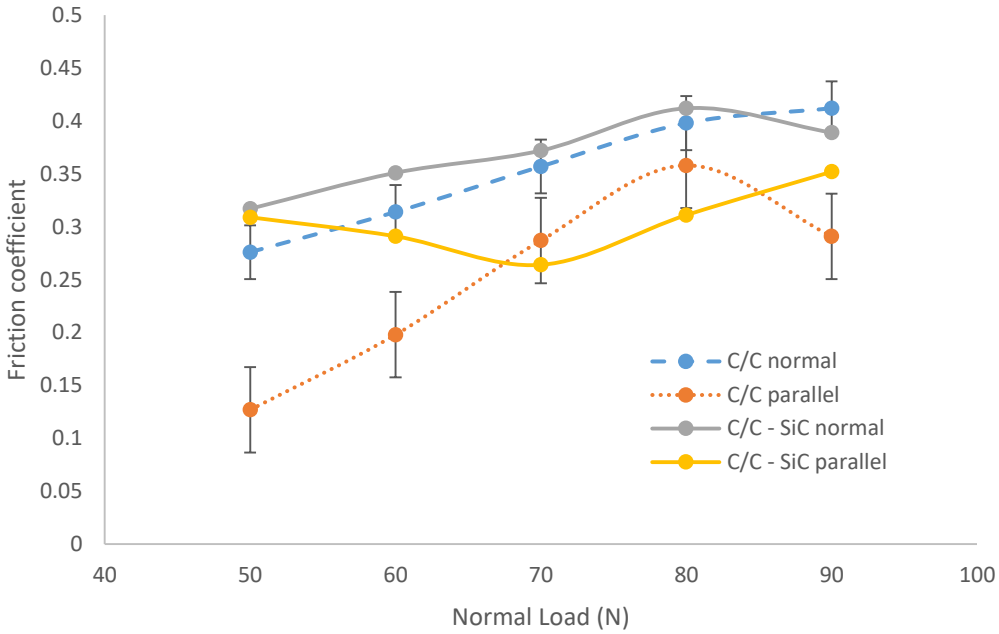


Fig. 3.22. Variation of friction coefficient with normal load of C/C normal, C/C parallel, C/C-SiC normal and C/C-SiC parallel composites.

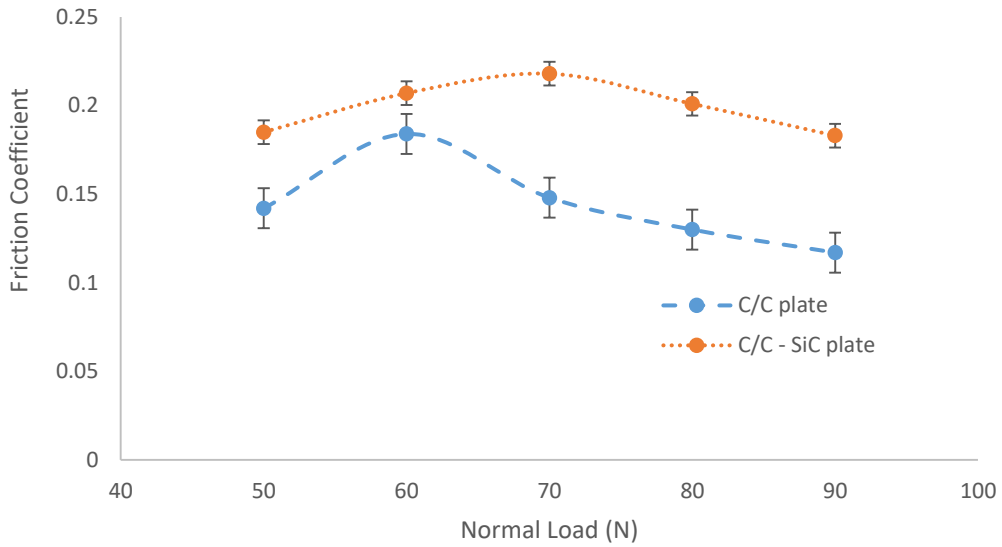


Fig. 3.23. Variation of friction coefficient with normal load in non-conformal hertzian contacts for C/C and C/C-SiC plate.

In the case of non-conformal hertzian contacts, the friction coefficient of C/C-SiC composites was higher as compared to C/C composites as can be observed in Fig. 3.23. However friction coefficient for both composites first increased with an increase in load and after that decreased. The friction coefficient of C/C-SiC composite showed less sensitivity to load as compared to C/C composite. This was due to an early increase in real contact area due to early wear of C/C composites with the increase in load.

### 3.5.2.2. Wear Behaviour

Fig. 3.24 shows the variation of wear loss with the load. It was observed from Fig. 3.24 that wear loss of C/C normal composites was highest at low loads in reciprocating sliding whereas C/C-SiC parallel showed highest wear loss at high loads. The wear loss of C/C

parallel and C/C-SiC parallel increased with increase in load whereas C/C normal and C/C-SiC normal showed opposite trends.

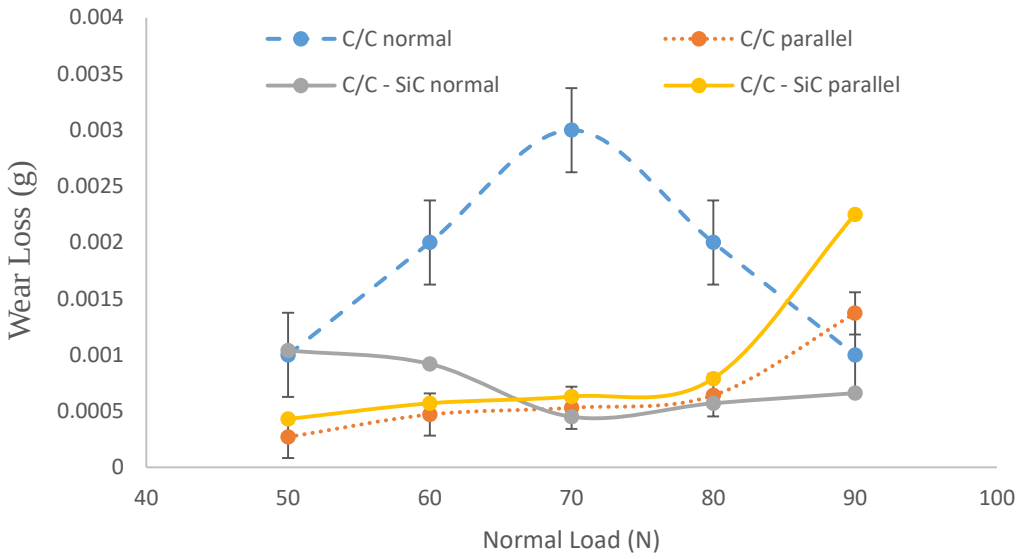


Fig. 3.24. Variation of wear loss with normal load of C/C normal, C/C parallel, C/C-SiC normal and C/C-SiC parallel composites.

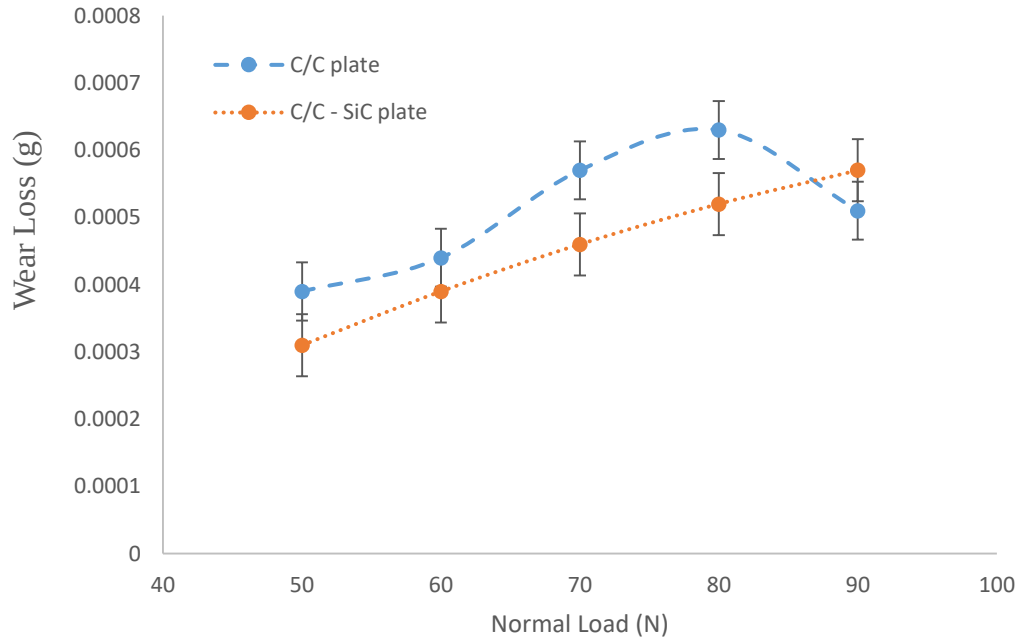


Fig. 3.25. Variation of wear loss with normal load in non-conformal hertzian contacts for C/C and C/C-SiC plate.

It can be observed from Fig. 3.25 that wear loss of C/C composite was more as compared to C/C-SiC composite in non-conformal hertzian contacts. C/C-SiC composites showed an increase in wear loss with the increase in load whereas wear loss of C/C composites first increased and after that decreased with increase in load.

### 3.5.2.3. Discussion

It was observed that fluctuation in friction coefficient for composites with normal orientation of laminates was more as compared to the parallel orientation of laminates whether it was C/C composites or C/C-SiC composites. This was attributed to the more surface porosity in case of parallel orientation of laminates. As the time of sliding increased, wear debris filled the surface pores and formed the smooth surface in case of parallel orientation of laminates. Thus, the number of cycles for stabilization of friction coefficient in case of parallel orientation of laminates was less. The friction coefficient of composites with normal orientation of laminates was more as compared to the parallel orientation of laminates. The friction coefficient of C/C normal first increased with time and after some time, it decreased. The increase was attributed to the rise in temperature which in turn increased the adhesion and abrasion of contact conjunctions and asperities on the contact surface [124]. However, the formation of friction film after some time due to pulverization of wear debris decreased the friction coefficient of C/C normal. The friction coefficient of C/C-SiC normal didn't change much with time due to the presence of hard SiC particles which led to the disruption of any friction film formed on the surface.

The friction coefficient of composites with normal orientation of laminates generally increased with an increase in load. The increase was due to the deeper penetration of

asperities as the load was increased. Some cracks were developed on the surface of composites with normal orientation of laminates as can be observed from Fig. 3.26(a) and 3.26(b).

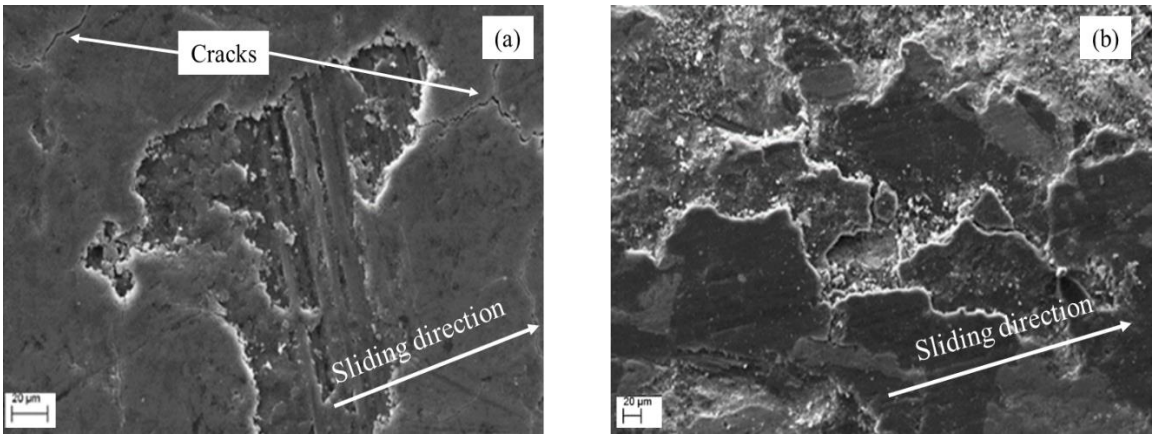


Fig. 3.26. SEM images showing composites tested at 70 N normal load (a) C/C normal, and (b) C/C-SiC normal.

The development of cracks was due to change in the direction of sliding in the reciprocating motion. Generally, these types of cracks are not much observed in unidirectional sliding because, in case of unidirectional sliding, repeated flexion of asperities in the opposite direction doesn't occur. The cracks loosen the matrix material from the contact surface. Further increase in load decreased the friction coefficient in the case of C/C-SiC normal. This was due to the presence of hard SiC particles which were ejected from the surface due to repeated flexion and acted as third body.

C/C composites showed the opposite trend for friction coefficient as compared to C/C-SiC composites when loaded in a parallel orientation of laminates. As the load was increased, deeper penetration of asperities led to an increase in friction coefficient in case of C/C

parallel. Fig. 3.27(a) shows C/C parallel tested at 80 N load. Wear debris from carbon matrix as well as from carbon fibers can be observed. The size of fibre fragments in wear debris was very small.

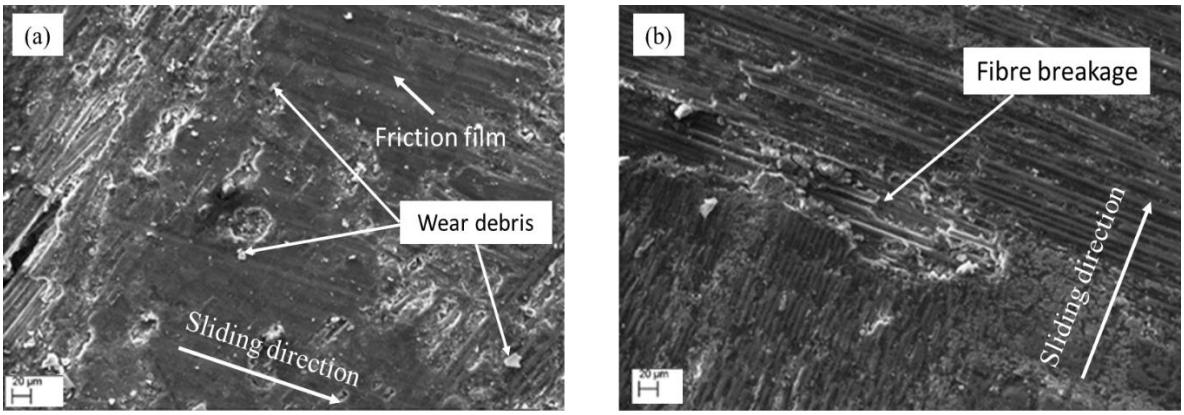


Fig. 3.27. SEM images showing (a) C/C parallel tested at 80 N, and (b) C/C-SiC parallel tested at 70 N.

At high loads, pulverization of debris led to the formation of friction film which decreased the friction coefficient. In the case of C/C-SiC parallel, hard SiC particles in wear debris acted as third body particles between composite and counterface. SiC particles are hard to pulverize even at high loads. This led to a decrease in friction coefficient. Fig. 3.27(b) shows C/C-SiC parallel tested at 70 N load. It was observed that the surface was smooth in case of C/C-SiC parallel as compared to C/C parallel. Fibre breakage at some regions was observed In the case of reciprocating sliding, sliding occurs in a very confined region. Wear debris generated generally get entrapped in the sliding region. Thus repeated sliding over the same wear debris led to embedment of hard SiC particles in the counterface at high loads which in turn increased the friction coefficient.

It was observed that at high loads, the friction coefficient of C/C composites was almost equal to the friction coefficient of C/C-SiC composites with normal orientation of laminates. However, the difference was large in case of composites loaded with a parallel orientation of laminates. The friction coefficient of composites with normal orientation of laminates was more as compared to composites with a parallel orientation of laminates in reciprocating sliding. This was attributed to the early formation of a smooth surface in case of composites with the parallel orientation of laminates.

In the case of non-conformal hertzian contacts, the fluctuation in the friction coefficient of C/C composites was large as compared to C/C-SiC composites. C/C-SiC composites showed a higher friction coefficient as compared to C/C composites. In the case of non-conformal hertzian contacts, the stress induced was localized and very high at the same loads when compared with low conformity contacts.

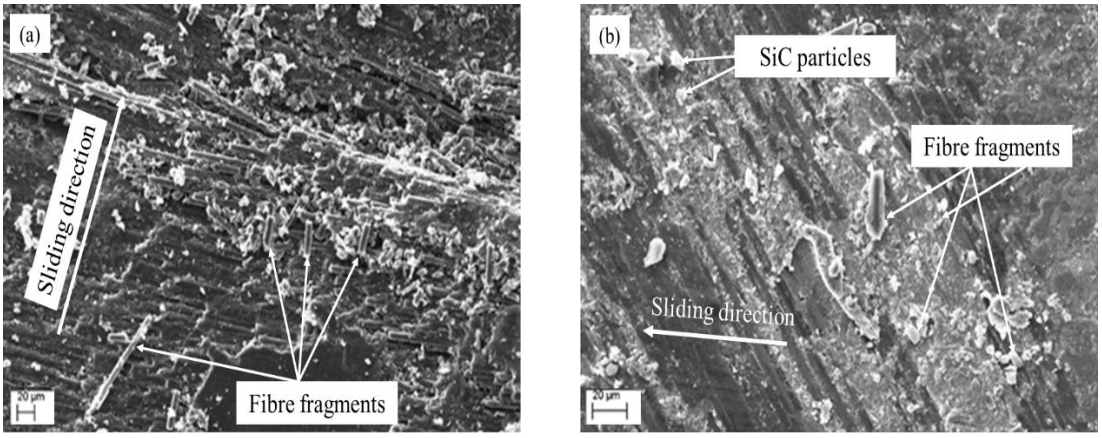


Fig. 3.28. SEM images showing composite tested at 70 N in non-conformal hertzian contacts (a) C/C composite, and (b) C/C-SiC composite.

These very high and localized stresses led to the fracture of fibers in small fragments as can be observed in Fig. 3.28(a). These fragments along with the wear debris from the matrix easily formed friction film due to high localized stresses and led to a decrease in friction coefficient at high loads. However, in the case of C/C-SiC composites, the wear debris was mainly comprised of SiC particles and some fiber fragments as observed in Fig. 3.28(b).

Due to very high stresses, these SiC particles tend to embed in the counterface. But the contact area was very small due to which only a few particles embedded in the counterface. SiC particles nearby contact area partially resisted the motion as these particles were entrapped in the sliding region. Thus, increase in load didn't significantly affect the friction coefficient of C/C-SiC composites in non-conformal hertzian contacts.

In the case of non-conformal hertzian contacts, the friction coefficient was lower as compared to low conformity contacts. This was due to low asperity interaction and early formation of friction film in case of non-conformal hertzian contacts.

It was observed that wear loss increased with increase in load in case of composites loaded with the parallel orientation of laminates. However, C/C composites showed the opposite trend as compared to C/C-SiC composites when loaded in normal orientation of laminates.

In the case of C/C normal, the developed cracks loosen the matrix material. Thus the asperities from the counterface interacted with the matrix material in between the laminas due to repeated flexion in the opposite direction. Partial crack propagation also occurred in between the laminas. This led to the ejection of the matrix from in between the laminas. This increased the wear loss. However, at high loads, the generated wear debris pulverized and decreased wear loss. In the case of C/C-SiC normal, hard SiC particles prevented the direct contact of composite and counterface which decreased the wear loss. In the case of C/C-SiC

parallel, the rise in temperature close to the friction surface lowered the compressive and interlaminar shear strength which increased the wear loss with the increase in load [125]. The rise in temperature was more in case of C/C-SiC parallel as compared to C/C-SiC normal due to the difference in thermal conductivity of carbon fibers in the longitudinal and axial direction and thermal conductivity of SiC particles [169]. Wear loss of C/C composites in non-conformal hertzian contacts first increased with an increase in load and decreased at 90 N load whereas C/C-SiC composites showed an increasing trend. The increase of wear loss in C/C composites was attributed to the increase in abrasive wear loss at high loads. As the load was increased further, the high localized pressure led to an increase in temperature at the local position which in turn led to graphitization at that position. This increased plasticity of carbon matrix and formation of smooth friction film took place which decreased the wear loss [170]. For C/C-SiC composites in non-conformal hertzian contacts, embedment of SiC particles in the counterface was easy due to high localized stresses. Thus counter surface embedded with SiC particles abraded the composite and increased wear loss with the increase in load.

In case of unidirectional sliding, wear loss for non-conformal hertzian contacts is generally more than low conformity or fully conformal contacts. But in case of reciprocating sliding, opposite occurred. This was due to the entrapment of wear debris in between the interacting surfaces due to small stroke length.

### 3.5.3. Conclusions

#### 3.5.3.1. Unidirectional Sliding

The important results obtained from the present investigation on C/C and C/C-SiC composites in unidirectional sliding are as follows:-

1. The friction behaviour of composites with parallel orientation of laminates was more stable as compared to normal orientation of laminates whether it was C/C or C/C-SiC composites due to easy formation of smooth surface with time because of more surface porosity in case of parallel orientation of laminates.
2. When the load was increased, C/C-SiC composites showed same friction behaviour for both orientations due to presence of hard SiC particles which minimized the effect of friction film, whereas C/C composites showed opposite behaviour for different orientation of laminates i.e., parallel and normal orientation.
3. C/C and C/C-SiC composites having same orientation of laminates yielded almost same friction behaviour with increase in sliding velocity.
4. The friction coefficient of C/C-SiC composites didn't vary much with change in surface conformity, but a large reduction was observed in case of C/C composites for non-conformal contacts due to its low hardness as compared to C/C-SiC composites.
5. Composites with parallel orientation of laminates showed less wear loss for both composites i.e., C/C and C/C-SiC composites, whereas nature of wear behaviour didn't change much with variation in laminate orientation when the load was increased.
6. At low sliding velocities, wear loss of composites with normal orientation of laminates was more whereas at high sliding velocities, composites in parallel orientation of laminates showed more wear loss.
7. C/C composites showed almost 20 to 80 times increase in wear loss in case of non-conformal hertzian contacts when compared to low conformity contacts at same load

with parallel orientation of laminates. C/C-SiC composites showed up to 10 fold increase in wear loss in non-conformal hertzian contacts.

### 3.5.3.2. Reciprocating Sliding

The important results obtained from the present investigation on C/C and C/C-SiC composites in reciprocating sliding are as follows:-

1. The friction behavior of C/C and C/C-SiC composites was more stable when loaded with parallel orientation of laminates in reciprocating sliding.
2. Friction coefficient of composites with normal orientation of laminates was generally more as compared to composites with parallel orientation of laminates. Cracks were developed in case of normal orientation of laminates due to repeated flexion of asperities in opposite direction.
3. In reciprocating sliding, wear debris got entrapped in the sliding region which made its tribological behavior different from unidirectional sliding.
4. Tribological behavior of C/C and C/C-SiC composites in non-conformal hertzian contacts was governed by low asperities interaction and high local stress.
5. Wear loss in case of non-conformal hertzian contacts was less as compared to low conformity contacts due to entrapment of debris. This behavior was opposite to the general wear behavior shown in unidirectional sliding.